Scanning Microscopy

Volume 7 | Number 3 Article 7

9-20-1993

Local Susceptibility Against Soft Errors in Dynamic Random Access Memories (DRAMs) Analyzed by Nuclear Microprobes

H. Sayama
Osaka University

M. Takai
Osaka University

H. Kimura
Mitsubishi Electric Corporation

Y. Ohno
Mitsubishi Electric Corporation

S. Satoh
Mitsubishi Electric Corporation

Scanning Microscopy, Vol. 7, No. 3, 1993 (Pages 825-835) 0891-7035/93$5.00+.00
Scanning Microscopy International, Chicago (AMF O'Hare), IL 60666 USA

LOCAL SUSCEPTIBILITY AGAINST SOFT ERRORS IN DYNAMIC RANDOM ACCESS MEMORIES (DRAMs) ANALYZED BY NUCLEAR MICROPROBES

H. Sayama[1] M. Takai[1]*, H. Kimura[2], Y. Ohno[2] and S. Satoh[2]

[1] Faculty of Engineering Science and Research Center for Extreme Materials, Osaka University, Toyonaka, Osaka 560, Japan
[2] LSI Research and Development Laboratory, Mitsubishi Electric Corporation, Itami, Hyogo 664, Japan

(Received for publication May 8, 1993, and in revised form September 20, 1993)

Abstract

A novel evaluation technique for soft errors in Mbit DRAMs (dynamic random access memories) has been developed using a 400 keV proton microprobe system. This technique, which is called soft error mapping, consists of a bit-state mapping image and a secondary electron mapping image, and can reveal the correlation between the incident position of protons and susceptibility against soft errors in DRAMs. Soft errors are found to be induced by proton incidence at 400 keV within about 6 μm around the memory cell in the case of DRAMs with a conventional well. The susceptible area against proton incidence is much larger than the memory cell size. It is found that the area within 4 μm around the memory cell is, in particular, highly sensitive to 400 keV protons. A threshold dose to radiation hardness is estimated by deterioration of the DRAMs during soft error mapping. A buried barrier layer, formed by high-energy ion-implantation, was found to control the charge collection of induced carriers and to suppress soft errors by 400 keV proton microprobes.

Key Words: Dynamic random access memory, soft error, single event upset, nuclear microprobe, soft error mapping, secondary electron mapping, radiation hardness, buried barrier layer, retrograde well, high-energy ion-implantation.

***Address for correspondence**:
Mikio Takai
Faculty of Engineering Science, Osaka University,
Toyonaka, Osaka 560, Japan
Phone: +81-6-844-1151
Fax: +81-6-857-7664

Introduction

Trends in DRAM

Soft errors are recognized as a serious problem of future memory devices. For instance, memory cells in a dynamic-RAM (DRAM) are further shrunk and integrated with scaling laws [4]. As the metal-oxide-silicon (MOS) capacitor, a significant part of a memory cell in DRAMs, is also shrunk, the stored charge in the capacitor representing a bit-state is drastically decreased. The memory capacitor with decreased stored charges becomes much more sensitive to external electronic noise, such as hot carriers [1], alpha-particle irradiation emitted from device packages and wiring [12], and cosmic rays [14]. In the conventional environment, soft errors in DRAMs are caused by alpha-particles at an energy of less than 5 MeV that create 1.4×10^6 electrons more than the stored charges in the dynamic memory cell. Some 3-dimensional capacitor structures were invented to keep constant stored charges against the scaling law, for examples, the trench capacitor [22] and the stacked one [11]. Moreover, charge collection can be controlled by modifying the substrate, as in the case of silicon-on-insulator (SOI) structures [21], silicon-implanted-oxygen (SIMOX) wafers [10], epitaxial wafers [9] and buried barrier-layers formed by high-energy ion-implantation [24]. However, the adoption of lower bias voltages makes memory cells more sensitive in spite of such new structures.

Soft error mechanism in DRAM

Two modes of soft errors in DRAMs are considered to be distinguished by changing cycle times for the operation; a cell mode [12] and a bit-line mode [25]. Figure 1 shows the cell mode soft error which means the loss of the bit-state in a memory cell. The electrons created by an alpha-particle along its track are collected in a storage capacitor. The bit-state is preserved in the case of the initial bit-state '0' corre-

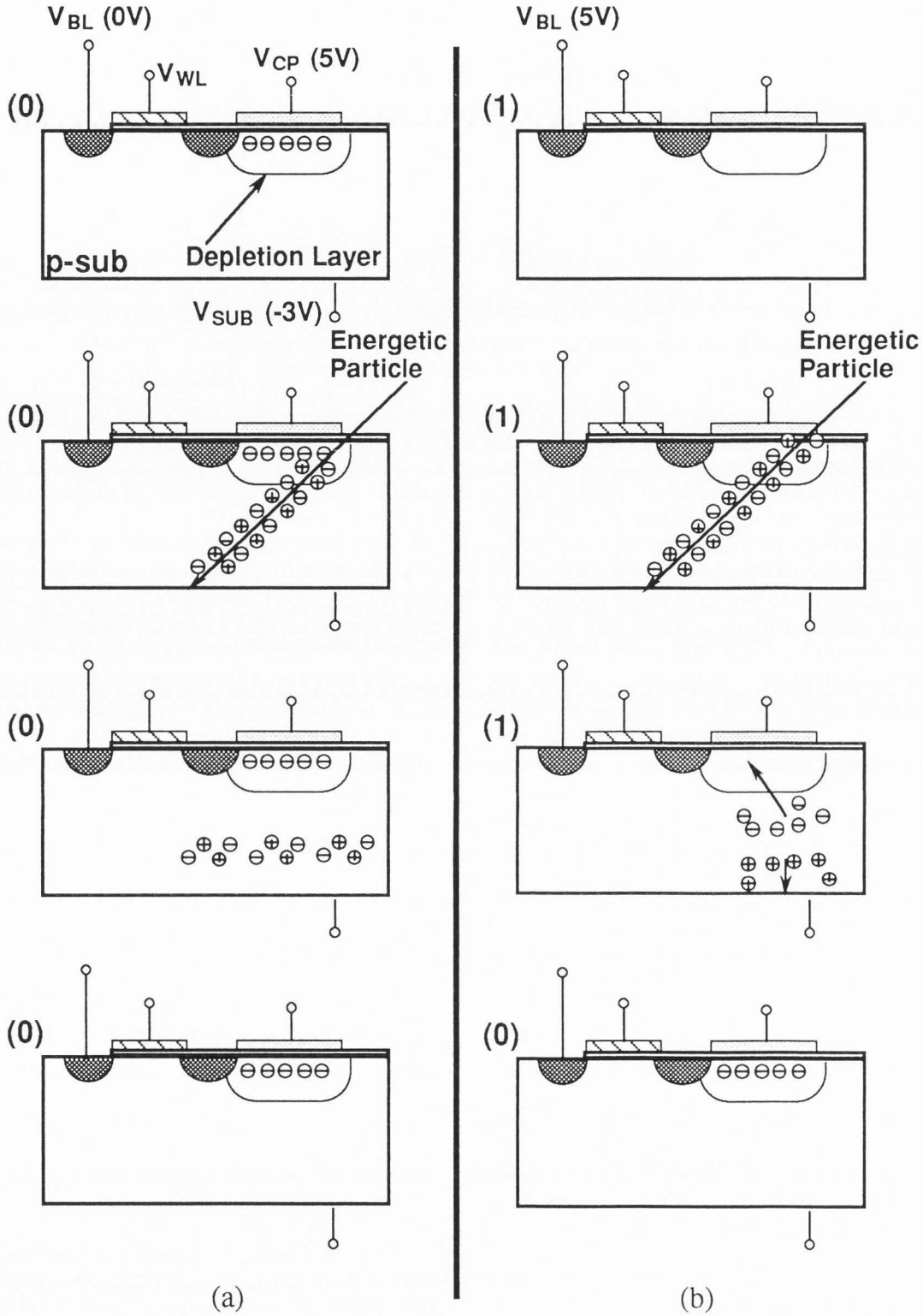

Figure 1 Dynamics of cell-mode soft errors in p-type Si induced by an energetic particle. The initial bit-state is '0' in (a) and '1' in (b). Cell mode soft errors take place only in (b). V_{SUB}, V_{WL}, V_{BL} and V_{CP} mean biases applied to substrate, word-line, bit-line and capacitor, respectively.

sponding to the capacitor filled with electrons (Fig. 1a). On the contrary, the upset state '0' is produced by the collection of many electrons in the initial bit-state '1' corresponding to the capacitor without electrons (Fig. 1b).

On the other hand, bit-line mode soft errors are considered to be induced by the collection of electrons to bit-line contacts in a floating time during a read operation because bit-line mode errors are inversely proportional to cycle times. All the two types of upsets, '1' to '0' and '0' to '1', can be induced in the bit-line mode because an alpha-particle hits the contacts of a bit-line and of the dummy bit-line.

Thus, these two modes of soft errors would depend on the device element positions to which created electrons are collected but share the same charge collection mechanisms. The electrons created by an alpha-particle diffuse and drift within a depletion layer. Some electrons are collected by funneling [8], in which the depletion layer spreads along the track of an energetic particle in the shape of a funnel because the created electron-hole pairs force to cancel the applied substrate potential.

Soft error measurement

Soft error immunity has conventionally been evaluated using energetic particles from a radioactive source [2] or an accelerator [27]. Figure 2 shows the schematic view of a soft error evaluation method using a radioactive source. The radiation source such as an americium or a thorium source is located over memory devices. This method can statistically manifest soft error immunity of the whole devices. Soft errors only in a single device element, however, cannot be evaluated because the incident position of the particles in a device chip is random. The incident angle of the particles is also random. Therefore, a new technique has been developed to clarify a hitting position and an angle to the device surface of a radiation particle.

Microprobe application to soft error measurement

Nuclear microprobes, high energy focused ion beams, have been developed for non-destructive analyses technology in archaeology, biology and semiconductor, using particle-induced X-ray-emission (PIXE) and/or Rutherford-backscattering (RBS) [23]. Nuclear microprobes will be a powerful analytical tool for local susceptibility of soft errors because the incident position and angle to the devices can be easily controlled. Microprobe techniques were once

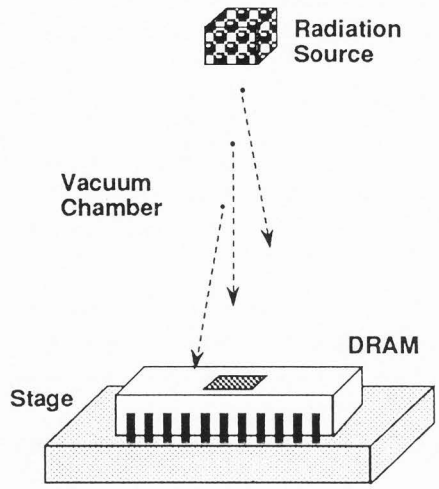

Figure 2 Schematic view of a soft error evaluation method using a radioactive source.

applied for the evaluation of soft errors in the early stage of DRAM generations. Campbell et al. investigated 16 Kbit DRAMs using He^+ microprobes collimated by a pin-hole slit with 2.5 μm diameter [3], and Geppert et al. also investigated 2 x 256 Kbit DRAMs using He^+ microprobes [6]. However, the exact incident position of the microprobes was not unambiguously identified because the irradiated position was determined by movements of the mechanical stage with a low accuracy in both experiments. Hence the exact correlation between the incident position of energetic particles and soft errors could not be obtained. Recently, nuclear microprobes with a spot size of about 1 μm, almost as small as cell sizes of Mbit DRAMs, have been developed using precise quadrupole lenses. Moreover, nuclear microprobes can provide mapping images such as a secondary electron image by raster-scanning the focused beam. Such small scanning microprobes have been applied to a soft error evaluation in 16 Kbit static-RAMs (SRAMs) by Horn et al. [7]. The application of the nuclear microprobe techniques to DRAMs is more difficult than that to SRAMs because of the dynamic operations. The bit states of SRAMs are kept and are slowly read out after probe irradiation, while DRAMs require both refresh operation and rapid reading out. Moreover, a huge apparatus is required for operation of Mbit DRAMs if all the bit-states are monitored.

In this study, a one-bit memory cell was operated because of the ease in dynamic operation, and proton microprobes at 400 keV were applied to soft error

evaluations of Mbit DRAMs. The susceptible area of a single device was investigated by raster-scanning the microprobes with various spot sizes. The threshold dose for a radiation hardness is also determined to avoid deterioration of the exposed DRAMs during soft error mapping measurements. Additionally, the dependence of soft errors upon well structures of the DRAMs was investigated by proton microprobes.

Experimental Procedures

Soft error mapping

The analytical system, which has originally been developed for 3-dimensional analysis using micro-RBS, was modified for soft error evaluations in DRAMs [17]. Ion beams from a 500 kV Disktron accelerator [23] are focused to about 1 μm by quadrupole magnets. The focused ion beams were raster-scanned over the targets fixed on the 5-axis goniometer after the area to be irradiated was roughly moved by the goniometer. The bit-state of only one particular cell was operated and monitored. Two kinds of mapping images, a bit-state mapping image and a secondary electron mapping image, were obtained for the same irradiated area by two beam scans, respectively. The information in a pixel of a bit-state mapping image indicates at least one bit-state change from '1' to '0' of the monitored cell when the microprobe are irradiated to the pixel. On the other hand, the secondary electron image indicates the exact location in the DRAM chip corresponding to the irradiated area in the bit-state mapping image. The location of sensitive positions in the DRAMs against soft errors can be revealed using the soft error mapping produced by overlapping the bit-state mapping image, the secondary electron mapping image and the Al wiring pattern around the monitored cell. Thus, the correlation between the microprobe hit position and the occurrences of soft errors in a single memory element can be clearly identified.

Susceptibility mapping

Since the change in bit-states could be monitored in a bit-state mapping image, further improved susceptibility mapping image was recently introduced [16]. The susceptibility mapping image indicates the degree of susceptibility in an irradiated pixel, and depends upon wiring structures of the measured devices and the charge collection in the substrate. The measurement procedure of a susceptibility mapping image is the same as the bit-state mapping image except for the signal processing. Only '1' bit-state pulses of output were counted during the beam dwell time (10 ms) in each irradiated pixel while '1' bit-state is repeatedly written and read in the monitored cell in every cycle (1 μs in this study). The output pulses of 10,000 can be counted in each pixel if no soft errors take place. The reduction of the count consequently manifests susceptibility against soft errors in each irradiated pixel. Thus, local susceptibility against soft errors in DRAMs was investigated by a susceptibility mapping image with nuclear microprobes.

Measured DRAMs

DRAMs with a capacity of less than 4 Mbit have already been in the market, while a first generation of 16 Mbit DRAMs is being prepared for mass production. In this study, soft error immunity was investigated using test element group (TEG) chips for 16 Mbit DRAMs which are constructed with stacked capacitors, folded bit-lines and gate electrodes with a length of 0.7 μm. The area of one memory cell is about 1 x 2 μm^2. The following bias voltages were applied; 5 V to power supply (Vcc), -3 V to the substrate and 2.5 V to the capacitor. The passivation layer was locally removed to obtain a clear probe-induced secondary electron image. Consequently, the overlaid layers on the substrate have a thickness of 2.8 μm after removal of the passivation layer. Only one particular monitored cell was operated after the following timing chart. Writing and reading processes were repeated every 1 μs (cycle time). The writing '1' to the monitored cell plays the role of a refresh operation. The interval in one cycle is 350 ns between the end of a write process and the beginning of a read process. Soft errors are induced by charge carriers created by energetic particles incident to the target devices in this interval.

Probe characteristics

In this study, 400 keV proton microprobes with a normal incidence to DRAMs were selected for a soft error evaluation because 400 keV He^+ cannot reach the substrate of the measured DRAMs through a thick overlaid layer. The energies of protons decrease to about 125 keV when they reach the substrate. The protons stop at a depth of about 1.1 μm beneath the surface of the substrate. The amount of electron-hole pairs, created along the track of a proton, depends on the predominant electronic stopping power. The electronic stopping powers of protons at an initial energy of 400 keV and of helium ions at that of 5 MeV are shown in Fig. 3. The energy deposited by a single proton is about two times higher than that of an alpha-particle in the region between surface and the projected ranges of protons. A single proton creates

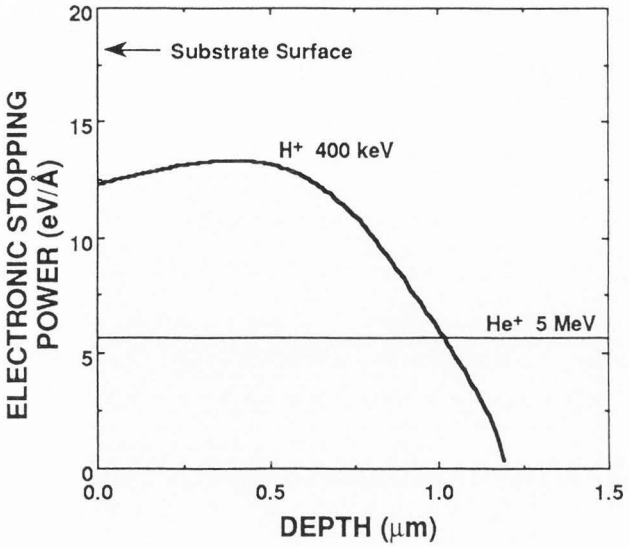

Figure 3 The electronic stopping power of protons with an initial energy of 400 keV. The electronic stopping power of helium ions at 5 MeV is also calculated.

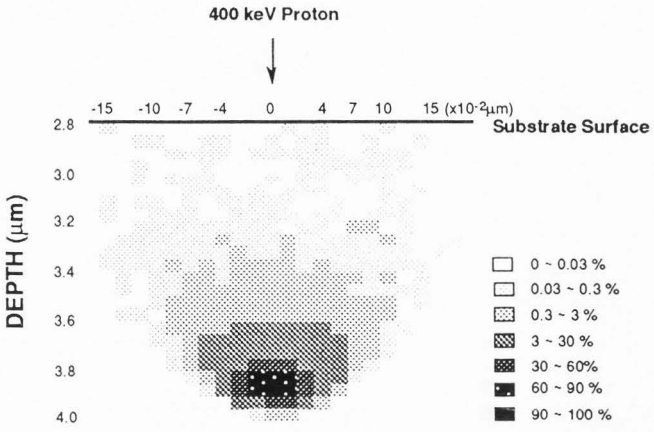

Figure 4 Two-dimensional concentration profile of 400 keV protons in the DRAM simulated by a TRIM Monte Carlo code.

about 3.5 x 10^4 electrons assuming that the energy requirement to create one electron-hole pair is 3.6 eV [15]. Multiple protons contribute to a soft error and create many electron-hole pairs near the surface under the conditions in this study. Proton microprobes with square spot sizes of about 4 x 4, 2 x 2 and 1 x 1 μm^2 were used for the measurement. Figure 4 shows the two-dimensional concentration profile of 400 keV protons in the DRAM calculated using a TRIM Monte Carlo code [26]. The lateral beam straggling of about 0.2 μm is much smaller than the probe spot sizes. The regions in which soft errors take place are thus assumed to depend on the incident position and spot size of the probe beam.

Results and Discussion

Beam spot size dependence

An Al wiring pattern on the top layer near the monitored cell of the measured DRAMs is shown in Fig. 5a. Open rectangles are a part of the memory cell array, and a solid one indicates the monitored cell at the corner of the memory array. Figure 5b shows a bit-state mapping image analyzed by 400 keV proton microprobes with a spot size of 4 x 4 μm^2 at a current of 80 pA. The microprobe was irradiated normal to the DRAM surface. The scanned area is a square of about 113 x 113 μm^2. The black marks reveal the occurrence of a soft error from '1' to '0' bit-state. Figure 5c indicates the secondary electron image of the same area as the bit-state mapping image. Figure 5d shows the soft error mapping image overlapped with Figs. 5a and 5b. Soft errors take place when the proton microprobe hits positions within 6 μm around the monitored cell as well as three other locations. The errors in the former represent cell mode soft errors including bit-line mode errors. The errors in the latter indicate bit-line mode errors and the locations correspond to the contacts of the bit-line, parallel to the top Al wiring, connected to the monitored cell. Thus, two modes of soft errors can be directly distinguished by the overlapped soft error mapping image.

Figure 6 shows the soft error mapping image using a microprobe with a spot size of 2 x 2 μm^2 at a current of 10 pA. It consists of an Al wiring pattern and a susceptibility mapping image. The depth of black tone in the susceptibility mapping image stands for the degree of susceptibility against 400 keV protons. Cell-mode soft errors are induced by the proton impact within 6 μm around the monitored cell. In particular, the most susceptible area against proton incidence is within 4 μm around the monitored cell.

Figure 7 shows the soft error mapping image using a microprobe with a spot size of 1 x 1 μm^2 at a current of 25 pA. As in the case of the probe spot size of 2 x 2 μm^2, cell-mode soft errors are induced by the

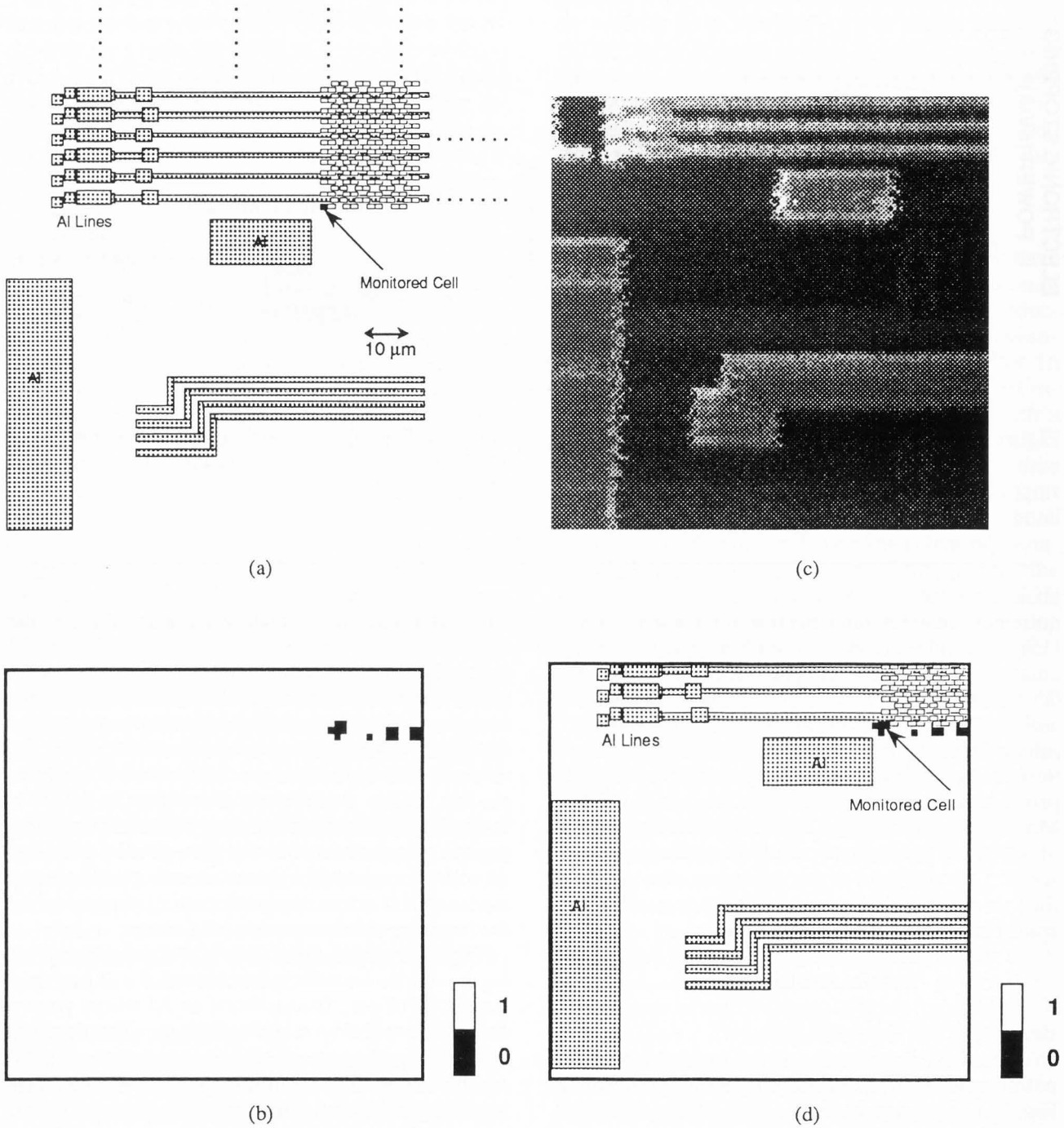

Figure 5 (a) A designed Al wiring pattern. The open rectangles are parts of memory cell array, and the solid one stands for the monitored cell. (b) Bit-state mapping image of the DRAMs. Proton microprobes at 400 keV were irradiated normal to the chips with a spot size of 4 x 4 μm^2 at a current of 80 pA. The square area of about 113 x 113 μm^2 is raster-scanned around the monitored cell. The black marks indicate soft errors of the monitored cell. (c) The secondary electron image to locate the exact cell area in the bit-state mapping image. (d) Soft error mapping image overlapped with Figs. 5a and 5b.

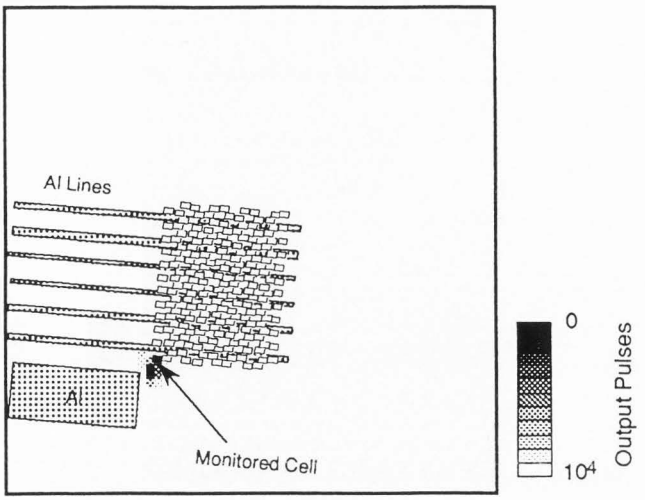

Figure 6 Soft error mapping image consisting of Al wiring patterns and a susceptibility mapping image, using a 400 keV proton microprobe with a spot size of 2 x 2 μm^2 at a current of 10 pA.

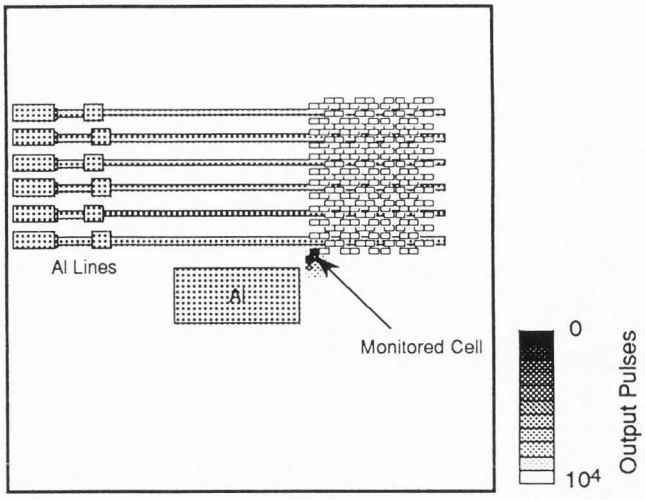

Figure 7 Soft error mapping image investigated by proton microprobes with a spot size of 1 x 1 μm^2 at a current of 25 pA.

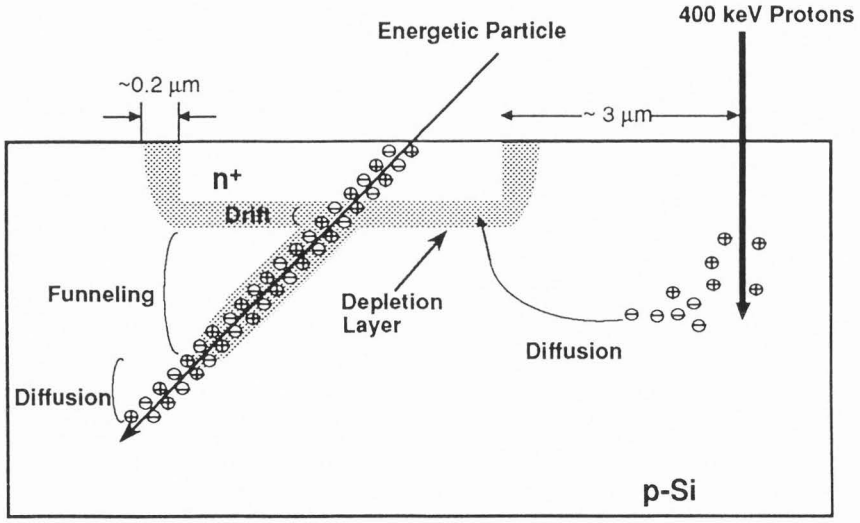

Figure 8 Schematic of charge collection in the DRAMs in soft error mapping measurements. All the charge collection mechanisms are also illustrated.

Table 1 Experimental conditions corresponding to Figs. 5, 6, 7, 9 and 11.

Figure No.	Beam spot (μm^2)	Current (pA)	Density (mA/cm^2)	Incident ions (ions/350ns)	Created carriers (electrons/350ns)
5	4 x 4	80	0.50	180	7.0×10^6
6,11	2 x 2	10	0.25	22	8.7×10^5
7	1 x 1	25	2.5	55	2.2×10^6
9	1 x 1	75	7.5	165	6.6×10^6

proton incidence onto the monitored cell within 6 μm, and the highly sensitive area is limited to an area of 4 μm around the monitored cell. According to the Figs. 5, 6 and 7, the susceptible area of the DRAMs against the proton incidence is found to be much larger than the memory cell size of about 1 x 2 μm^2 although the lateral width of the depletion layer of the memory cell is 0.2 μm. These results indicate that carrier diffusion is the predominant charge collection mechanism in this study shown in Fig. 8 because many charge carriers are created by 400 keV protons near the surface of the substrate. Thus, the susceptible area is considered to be independent of the probe spot sizes within the experimental range. Higher energy microprobes, which provide less carriers near surface, would presumably exhibit different results.

Table 1 shows the parameters in each experiment. The carriers created by the proton microprobes within the 350 ns in a read-write cycle, contribute to cell-mode soft errors. The number of created carriers in each impact exceed the critical charge of the memory cell (about 360000 electrons) and is estimated to be half of the stored charge. The exact critical charge could be determined by changing the probe current if the efficiency of charge collection were known. Bit-line mode soft errors can be observed only in Fig. 5, which suggests that bit-line mode soft errors depend upon the probe current. The protons impacting in the interval of the floating bit-line contribute to bit-line mode soft errors. Therefore, only high probe current of 80 pA would induce bit-line mode errors because the floating time of a bit-line is extremely short.

Radiation hardness

A high current density or a high dose rate of the microprobe will destroy memory cells during a soft error mapping measurement, and hence the radiation hardness of the devices should be investigated. Figure 9 shows the typical soft error mapping image for radiation hardness when the DRAMs were investigated by a proton microprobe with a spot size of 1 x 1 μm^2 at a current of 75 pA. After the microprobe was irradiated to the monitored cell, a write process was impossible. Some pulses corresponding to a bit-state '1' were observed after signal loss from the monitored cell. These pulses stand for the bit-line mode soft errors because of the high probe current. Current density, i.e., dose rate, is a significant factor in radiation hardness. Even in the case of the spot size of 1 x 1 μm^2 at a current of 25 pA in Fig. 7, the dose in the probe spot is 3.4 x 10^{14} ions/cm^2, which is high enough to evaluate the soft error immunity. However, in the case of Fig. 9, the dose of 1.0 x 10^{15} ions/cm^2 destroys the memory cell and is unsuitable for soft error measurements. It is found that the dose in the probe spot for a soft error evaluation should be less than 3.4 x 10^{14} ions/cm^2 using a 400 keV proton microprobe technique.

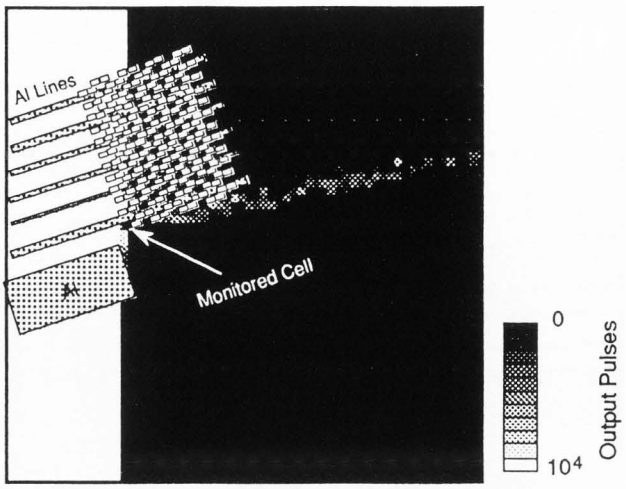

Figure 9 Soft error mapping image measured by a proton microprobe with a spot size of 1 x 1 μm^2 at a current of 75 pA. The monitored cell was deteriorated by the proton microprobe during the susceptibility mapping measurement.

Well structure

The modification of the substrate carrier profile, so called 'well engineering,' is expected to provide soft error immune structures which suppress charge carrier collection into the storage node of the devices. High-energy ion-implantation has been investigated and appears to be a powerful technique for well engineering [18, 19, 20, 24]. The buried layers or retrograde wells, formed by high-energy ion-implantation, are considered to be effective to soft errors and latch-up [5] because they act as a barrier against induced charge carriers, i.e., noise carriers. DRAMs with buried barrier layers were investigated using nuclear microprobe techniques for the confirmation of soft error reduction [13]. Figure 10 shows the cross-sectional view of the DRAM with two p^+-buried-layers. One layer for a retrograde well was formed by boron ion-implantation at an energy of 160 keV, and another deeper layer for a buried barrier was implanted with boron ions at an energy of 700 keV after LOCOS (Local Oxidation of Silicon) process. The implanted layers are located at a depth of 0.44 and 1.35 μm beneath the surface of the silicon substrate, respectively. Fig-

ure 11 shows the soft error mapping image of the DRAM in Fig. 10. The proton microprobe with a spot size of 2 x 2 μm^2 at a current of 10 pA was irradiated normal to the DRAM. There are no black marks in the mapping image, so no bit-state changes of the monitored cell from '1' to '0' occurred under the same probe condition as in the case of the DRAM with a conventional well in Fig. 6. The retrograde well suppresses the collection of noise carriers created by 400 keV protons to storage nodes, since the protons did not reach the deeper buried layer. Thus, the buried barrier layer was found to effectively suppress soft errors induced by 400 keV protons. However, charge collection efficiency cannot be clarified using a soft error mapping. A new method to investigate charge collection efficiency is being developed in this laboratory to optimize the depth and concentration of the buried layers formed by high-energy ion-implantation.

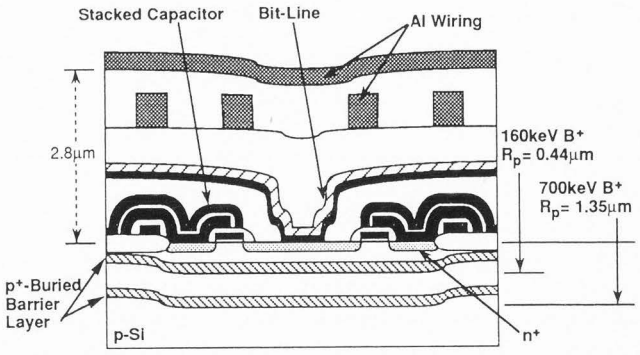

Figure 10 Cross-sectional view of the DRAM with two p^+-type buried layers. Implanted energies are 160 and 700 keV, their projected ranges are 0.44 and 1.35 μm in a silicon substrate, respectively.

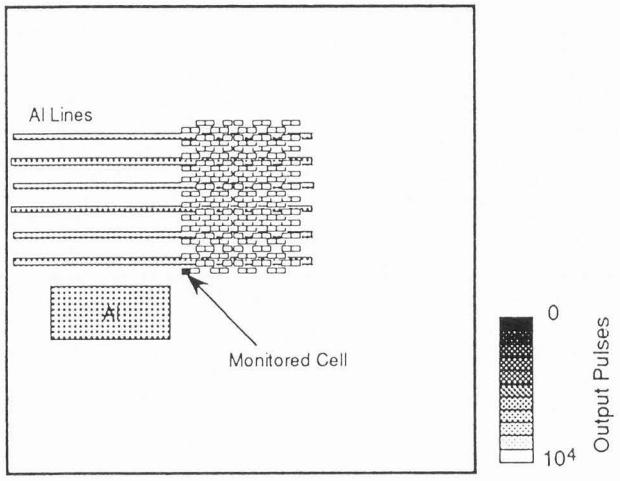

Figure 11 Soft error mapping image of the DRAMs with two p^+-type layers in Fig. 10. The proton microprobe with a spot size of 2 x 2 μm^2 at a current of 10 pA was irradiated normal to the DRAM. The probe condition is the same as in case of Fig. 6. No soft errors are observed.

Conclusions

Soft errors in 16 Mbit DRAM TEG chips could be evaluated by utilizing 400 keV proton microprobe beams as a radiation source. The correlation between incident position of protons and susceptibility against soft errors in one particular cell could be investigated, and hence cell mode and bit-line mode soft-errors were experimentally identified by the incident position of protons. The area susceptible against 400 keV protons exhibits little dependence upon the spot size of the probe beam. Soft errors in DRAMs are found to be induced by electron collection within 6 μm around the monitored cell. In particular, proton incidence within about 4 μm around the monitored cell easily induces soft-errors. This study indicates that the predominant collection mechanism of charge carriers into storage nodes is by carrier diffusion.

Beam induced radiation damage should be avoided when nuclear microprobe techniques are applied to soft error measurements. In order to avoid radiation damage, the dose in the probe spot for soft error evaluation should be less than 3.4 x 10^{14} ions/cm^2 using 400 keV proton microprobe beams.

No soft errors could be observed in a DRAM with a buried barrier layer for a retrograde well, formed by high-energy ion-implantation. The buried layers could suppress the collection of carriers created by 400 keV protons. The optimized carrier profile, modified by high-energy ion-implantation, would contribute to the suppression of soft errors induced by alpha-particle at about 5 MeV.

Acknowledgments

This work was supported by the System of Joint Research with Industry in 1992 (The Ministry of Education, Science and Culture and Mitsubishi Electric Corporation). The authors are indebted to S. Hara, M. Namba, H. Fujikawa, K. Kawasaki, and K. Mino of Osaka University and A. Kinomura of Governments Industrial Research Institute Osaka for their help in the measurement using nuclear microprobes and to H. Arima and H. Miyoshi of Mitsubishi LSI Research

and Development Laboratory for their helpful discussion.

References

1. Abbas SA, Dockerty RC (1975) Hot-carrier instability in IGFET's. Appl. Phys. Lett. **27**, 147-148.

2. Hidaka H, Arimoto K, Hirayama K, Hayashikoshi M, Asakura M, Tsukude M, Oishi T, Kawai S, Suma K, Konishi Y, Tanaka K, Wakamiya W, Ohno Y, Fujishima K (1991) A 34ns 16Mb DRAM with controllable voltage down converter. IEEE J. Solid-State Circuits **27**, 1020-1027.

3. Campbell AB, Knudson AR, Wolicki EA (1981) Investigation of soft upsets in MOS memories with a microbeam. Nuclear Instruments and Methods in Physics Research **191**, 437-442.

4. Dennard RH, Gaensslen FH, Yu HY, Rideout VL, Bassous E, Blanc AR (1974) Design of ion-implanted MOSFET's with very small physical dimensions. IEEE J. Solid State Circuits **SC-9**, 256-259.

5. Fang RCY, Moll JL (1984) Latchup model for the parasitic p-n-p-n path in bulk CMOS. IEEE Electron Devices **ED-31**, 113-120.

6. Geppert LM, Bapst U, Heidel DF, Jenkins KA (1991) Ion microbeam probing of sense amplifiers to analyze single event upsets in a CMOS DRAM. IEEE J. Solid State Circuits **26**, 132-134.

7. Horn KM, Doyle BL, Sexton FW (1992) Nuclear microprobe imaging of single event upsets. IEEE Trans. Nuclear Science **NS-39**, 7-12.

8. Hsieh CM, Murley PC, O'Brien RR (1981) A field funneling effect on the collection of the alpha-particle-generated carriers in silicon devices. IEEE Electron Device Letters **EDL-2**, 10-105.

9. Iwai H, Otsuka H, Matsumoto Y, Hisatomi K, Aoki K (1984) Comparison of intrinsic gettering and epitaxial wafers in terms of soft error endurance and other characteristics of 64k Bit dynamic RAM. IEEE Electron Device Letters **EDL-31**, 1149-1151.

10. Izumi K, Doken M, Ariyoshi H (1978) CMOS devices fabricated on buried SiO_2 layers formed by oxygen implantation into silicon. Electronics Letters **14**, 593-594.

11. Koyanagi M, Sunami H, Hashimoto H, Ashikawa M (1987) Novel high density, stacked capacitor MOS RAM. IEEE International Electron Device Meeting Technology Digest, 348-351.

12. May TC, Woods MH (1979) Alpha-particle-induced soft errors in dynamic memories. IEEE Trans. Electron Devices **ED-26**, 2-9.

13. Ohno Y, Kimura H, Sonoda K, Satoh S, Sayama H, Hara S, Takai M, Miyoshi H (1993) Soft-Error Study of DRAMs Using Nuclear Microprobe. In: International Reliability Physics Symposium, McPherson JW (eds), IRPS Publication Services, New York, 150-155.

14. Pickel JC, Blandford JT (1978) Cosmic ray induced errors in MOS memory cell. IEEE Trans. Nuclear Science **NS-25**, 1166-1171.

15. Ryan RD (1973) Precision measurements of the ionization energy and ITS temperature variation in high purity silicon radiation detectors. IEEE Trans. Nuclear Science **NS-20**, 473-480.

16. Sayama H, Hara S, Andoh H, Kimura H, Ohno Y, Satoh S, Takai M (1992) Soft-error immunity evaluation of DRAM using high-energy nuclear microprobe. Microelectronic Engineering **21**, 213-216.

17. Sayama H, Hara S, Kimura H, Ohno Y, Satoh S, Takai M (1992) New method for soft-error mapping in dynamic random access memory using nuclear microprobe. Jpn. J. Appl. Phys. **31**, 4541-4544.

18. Sayama H, Takai M, Akasaka Y, Tsukamoto K, Namba S (1989) Electrical evaluation of defects induced in silicon by high energy boron ion implantation. Jpn. J. Appl. Phys. **28**, L1673-1675.

19. Sayama H, Takai M, Namba S, Ryssel H (1991) Carrier concentration profiles by high-energy boron ion implantation into silicon. Nuclear Instruments and Methods in Physics Research **B59/60**, 1094-1097.

20. Sayama H, Takai M, Yuba Y, Namba S, Tsukamoto K, Akasaka Y (1992) Deep levels induced by high-energy boron ion implantation into p-silicon. Appl. Phys. Lett. **61**, 1682-1684.

21. Shichijo H, Malhi SDS, Shah AH, Pollack GP, Richardson WF, Elahy M, Banerjee S, Womack R, Chatterjee PK (1984) TITE RAM: a new SOI DRAM cell for Mbit DRAM's. In: 16 th Extended Abstracts of Solid State Devices and Materials, Namba S (eds), Business Center for Academic Societies Japan, Tokyo, 265-268.

22. Sunami H, Kure T, Hashimoto N, Toyabe T, Asai S (1983) A corrugated capacitor cell (CCC) for megabit-dynamic MOS memories. IEEE Electron Device Letters **EDL-4**, 90-91.

23. Takai M (1992) Formation of high energy microbeams and their application to microelectronics. Int. J. PIXE **2**, 107-128.

24. Tsukamoto K, Komori S, Kuroi T, Akasaka Y (1991) High-energy ion implantation for ULSI. Nuclear Instruments and Methods in Physics Research **B59/60**, 584-591.

25. Yaney DS, Nelson JT, Vanskike LL (1979) Alpha-particle tracks in silicon and their effect on dy-

namic MOS RAM reliability. IEEE Trans. Electron Devices **ED-26**, 10-16.

26. Ziegler JF, Biersack JP, Littmark U (1985) The stopping and range of ions in solids. Pergamon Press, New York 202-263.

27. Zoutendyk JA, Edmonds LD, Smith LS (1989) Characterization of multiple-bit errors from single ion tracks in integrated circuits. IEEE Trans. Nuclear Science **NS-36**, 2267-2274.

Discussion with Reviewers

R.F. Pease: What is meant by funneling in Fig. 8?
Authors: Funneling is a kind of charge collection mechanisms. Electron-hole pairs created by an energetic ion form dipoles because of the applied electric field, having an inverse field and resulting in cancellation of the applied field, which causes spreading of the depletion layer along the ion track in order to preserve the applied potential.

R.F. Pease: Explain exactly how Fig. 9 was obtained; what is the contrast mechanism?
Authors: The contrast of the susceptibility mappings corresponds to counts of pulses during beam dwell time of 10 ms. When microprobes are irradiated to a pixel in a mapping, 10^4 pulses can be counted if no soft errors take place. The pixel is painted in white. If soft errors take place, the number of counted pulses decreases and the pixel color becomes darker. In the case of Fig. 9, the microprobe, scanning from the top toward the bottom, begins at the left hand side of the mapping image. Before the irradiation of the monitored cell, no soft errors were observed (i.e., white pixels). When the microprobe was irradiated to the neighborhood of the monitored cell, soft errors were observed. The damaged monitored cell then could send no output pulses (i.e., dark pixels). However, some pulses were obtained when the microprobe was irradiated to the n^+ layer connected with the bit-line of the monitored cell (i.e., light contrast spots from the monitored cell to the right hand side of the mapping). The pulses correspond to the bit-line mode soft-error.

B. Doyle: Authors should address effect of beam halo.
Authors: Beam halo has an influence of the mapping resolution. The fwhm (full width at half maximum) value is used for the diameter of the probe. A few ions in beam halo during 1 cycle contribute to electron-hole pair generation. The carriers created by beam halo are sufficiently less than that of beam spot.

B. Doyle: What would have happened in Fig. 10 if higher energy protons had been used?
Authors: The deeper buried layer would effectively suppress the collection of charge created by higher energy protons. We are investigating the relation between well structures and higher energy protons.

N.W. Cheung: Authors may consider trying an angular dependence on soft error creating for retrograde wells. The side walls of these wells are lightly dope compared with the bottom.
Authors: The side walls immune against soft errors can be fabricated by combination of the retrograde well and channel stoppers which are heavily doped to the side walls. We are planning to investigate an angular dependence on soft errors to devices with a retrogade well and channel stoppers.

J.S. Williams: Did you investigate the beam current (dose rate) effects on soft error measurements?
Authors: Yes. Current densities in this study are listed in Table 1. The susceptible area is considered not to strongly depend on the beam current density.

J.S. Williams: Do you have any more details on radiation damage effects? Are you sure that the dose of 3×10^{14} cm^{-2} cause no long term effects?
Authors: No, we do not have any more details on radiation effects. We understand only that a soft error mapping should be measured under the condition of the dose less than 3×10^{14} cm^{-2}. The accumulation of the radiation damage would introduce device deterioration.